ARTICLE IN PRESS

Nature Communications

https://doi.org/10.1038/s41467-026-70455-7

Article in Press

Towards universal multi-dimensional parallelization communications by direct diverse fiber/3D/2D chip hybrid integration

Received: 20 October 2025

Accepted: 17 February 2026

Cite this article as: Li, K., Cai, C., Yan, G. *et al.* Towards universal multi-dimensional parallelization communications by direct diverse fiber/3D/2D chip hybrid integration. *Nat Commun* (2026). https://doi.org/10.1038/s41467-026-70455-7

Kang Li, Chengkun Cai, Guofeng Yan, Bing Han, Hang Chen, Guangze Wu & Jian Wang

We are providing an unedited version of this manuscript to give early access to its findings. Before final publication, the manuscript will undergo further editing. Please note there may be errors present which affect the content, and all legal disclaimers apply.

If this paper is publishing under a Transparent Peer Review model then Peer Review reports will publish with the final article.

ARTICLE IN PRESS

© The Author(s) 2026. **Open Access** This article is licensed under a Creative Commons Attribution-NonCommercial-NoDerivatives 4.0 International License, which permits any non-commercial use, sharing, distribution and reproduction in any medium or format, as long as you give appropriate credit to the original author(s) and the source, provide a link to the Creative Commons licence, and indicate if you modified the licensed material. You do not have permission under this licence to share adapted material derived from this article or parts of it. The images or other third party material in this article are included in the article's Creative Commons licence, unless indicated otherwise in a credit line to the material. If material is not included in the article's Creative Commons licence and your intended use is not permitted by statutory regulation or exceeds the permitted use, you will need to obtain permission directly from the copyright holder. To view a copy of this licence, visit http://creativecommons.org/licenses/by-nc-nd/4.0/.

ARTICLE IN PRESS

Towards universal multi-dimensional parallelization communications by direct diverse fiber/3D/2D chip hybrid integration

Kang Li[1,2,3,#] (kang@hust.edu.cn),

Chengkun Cai[1,2,3,#] (chengkuncai@hust.edu.cn),

Guofeng Yan[1,2,3,#] (2283246153@qq.com),

Bing Han[1,2,3](hanging010719@126.com),

Hang Chen[1,2,3] (17746722609@163.com),

Guangze Wu[1,2,3] (1539752347@qq.com),

Jian Wang[1,2,3*](jwang@hust.edu.cn),

[1] Wuhan National Laboratory for Optoelectronics and School of Optical and Electronic Information, Huazhong University of Science and Technology, Wuhan 430074, Hubei, China

[2] Hubei Optical Fundamental Research Center, Wuhan 430074, Hubei, China

[3] Optics Valley Laboratory, Hubei, Wuhan 430074, Hubei, China

[#] These authors contributed equally: Kang Li, Chengkun Cai, Guofeng Yan.

* Correspondence to: jwang@hust.edu.cn.

ARTICLE IN PRESS

ARTICLE IN PRESS

Abstract

Space-division multiplexing (SDM) is a promising technology for significantly increasing the capacity of a single fiber or waveguide. Various SDM fibers, including few-mode fibers (FMFs), multi-core fibers (MCFs), and orbital angular momentum fibers (OAMFs), demonstrate distinct advantages in fiber links, driving a prevailing trend toward their parallel utilization. Photonic integrated circuits extend SDM from long-distance fibers to chip-scale interconnects. However, mode-field mismatches between fibers and chips pose compatibility challenges. Here, we develop diverse fiber-chip couplers via fiber/3D/2D chip hybrid integration to achieve seamless “fiber-to-fiber” and “fiber-to-chip” mode-field conversions. Building on this, we integrate large-scale, multifunctional 2D silicon chips to construct a fiber-chip-fiber system compatible with FMF, MCF, OAMF, and single-mode fibers. This parallel communication successfully demonstrates 288 channels (8 spatial modes and 36 wavelengths) and 30-Tbit/s capacity. This work establishes a universal multi-dimensional parallelization communication architecture, paving the way for next-generation multi-dimensional data transmission and management.

Keywords: Space-division multiplexing; hybrid integration; multi-dimensional parallelization communications; orbital angular momentum.

ARTICLE IN PRESS

ARTICLE IN PRESS

Introduction

Optical communication is a critical part of global communication infrastructure, meeting the growing data demand[1–5]. While space-division multiplexing (SDM) technology utilizes orthogonal spatial/mode channels to significantly enhance fiber communication capacity [6–13], there has been no trend showing that a particular type of SDM fiber could dominate the field. Various types of fibers, such as few-mode fibers (FMF)[14–16], multi-core fibers (MCF)[17], orbital angular momentum fibers (OAMF)[18,19], and others, each has its respective advantages in specific domains. With the development of integrated photonic technologies[20], SDM is progressively extending from long-distance fiber-optic communication to short-distance waveguide transmission[21–23]. Multimode waveguide (MMW) can also multiply capacity by transmitting multiple orthogonal on-chip modes[24,25]. Therefore, in both the present and for the foreseeable future, compatible solution using multiple types of fibers and waveguides will remain the status quo in optical communications. To meet these challenges, universal interfaces and parallel communications supporting various fibers and waveguides have become more essential.

Integrated photonics can provide universal compact solutions. Despite the achievement of multi-dimensional data transmission integrated communication systems, conventional schemes still struggle to deliver the tailored interfaces and required data throughput while maintaining compact structure in multi-fiber/chip data transmission and processing scenarios. The challenges arise from two key aspects. Firstly, there are a significant shape/size mismatches in various fibers and waveguide, resulting in the inability of direct, efficient, and low-crosstalk interconnection of various spatial channels. The most convenient scheme to convert a spatially distributed field is to use the commercial spatial light modulators [26] and flexible fiber-optic devices [27], which, however, maintain their high performance with a large footprint. It is worth noting that fs-laser-inscribed silica chip offers excellent capability for manipulating complex two-dimensional optical field distributions within a compact footprint, owing to their intrinsic three-dimensional fabrication flexibility. However, since 3D photonic chips are typically fabricated in transparent dielectric substrates with waveguides embedded beneath the surface, integrating conductive electrodes deep within the structure remains a significant challenge. Additionally, electrode routing can introduce

optical losses and degrade device performance, thereby limiting the realization of advanced signal processing functions.

Another issue lies in the high-throughput data processing. Silicon photonics is considered to be an attractive signal processing platform owing to its high refractive index difference and complementary metal-oxide semiconductor compatibility. Recently, there have been notable advancements in the performance of silicon photonic signal processors, particularly in terms of throughput, reconfigurability, programmability, and multi-tasking. Some grating couplers and edge couplers have been proposed to successfully achieve coupling between fiber and chip[14,15,28–38], these couplers are only used to connect single-mode fiber (SMF) or FMF to silicon waveguides. Silicon MCF and OAMF couplers have rarely been reported. Therefore, different photonic chips possess complementary advantages and limitations. Although interfacing these strengths of two distinct chips presents a straightforward and commendable strategy for overcoming their respective shortcomings, until now, such a combination has typically relied on multiple single-mode fibers and fiber-optic components for interconnection, thereby undermining the anticipated merits of integrated photonics.

Here, we make a key step in combining these two essential integrated chips by the hybrid integration technologies, which not only achieve the compatibility with various fibers and waveguides, but also take advantage of 3D silica chip and 2D silicon chip in a compact form. Among them, the 3D silica chip provides efficient, low-crosstalk interfaces for various types of fibers and waveguides (OAMF, MCF, FMF, and MMW), therefore serving as a "bridge" between optical fibers and silicon chips. This bridging capability enables fiber-to-fiber and fiber-to-chip multimode field conversion. On this basis, by combining large-scale, multi-channel, multifunctional silicon chip, we construct a fiber-chip-fiber interconnection link equipped with OAMF, MCF, FMF, and SMF, featuring 288 optical management channels and a system capacity of 30 Tbit/s. This work provides an ideal compact platform to achieve mode manipulation and parallelization communications, and will accelerate the proliferation of SDM fibers and integrated photonics chips for the next generation of communication system.

Results

ARTICLE IN PRESS

Design and fabrication

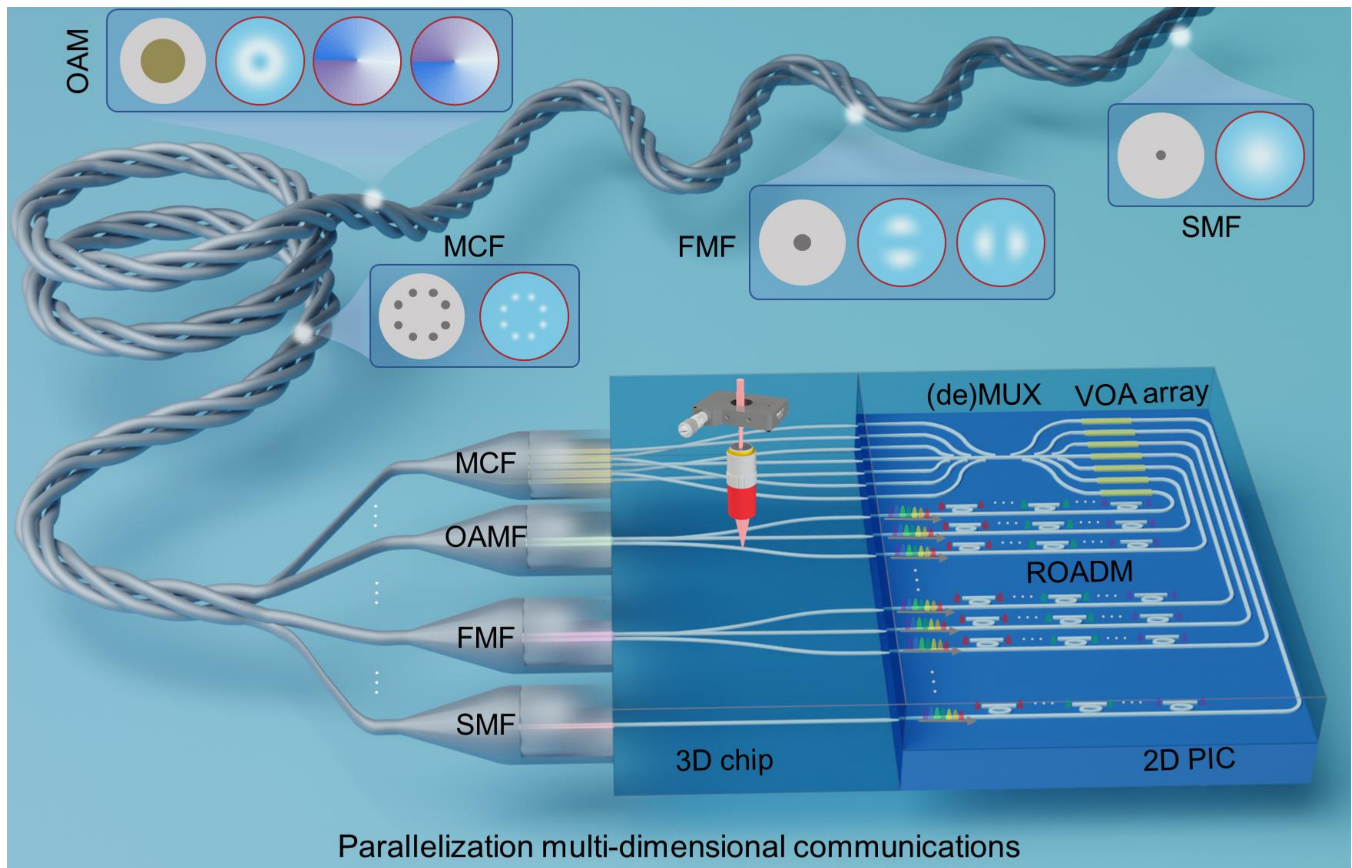

Fig. 1. Parallelization multi-dimensional communications in diverse space-division multiplexing fiber link using 3D/2D chip hybrid integration. Diverse fibers include SMF, MCF, FMF, and OAMF. The fs-laser inscribed 3D chip is used to tailor various I/O interface for fibers and chips. The silicon 2D chip is used to manage high-throughput signal. MCF: multi-core fiber; OAMF: orbital angular momentum fiber; FMF: few-mode fiber; SMF: single-mode fiber; VOA: variable optical attenuator; ROADM: reconfigurable optical add/drop multiplexer; PIC: photonic integrated circuit.

The proposed diverse parallel multi-dimensional communication is illustrated conceptually in Fig. 1. The design enables parallel data transport and management through multi-fiber, multi-chip, and multi-dimensional coordination. Multiple fibers including SMF, FMF, MCF, and OAMF, serve as the long-distance data transmission medium, supporting multiple wavelengths. Each fiber can be directly coupled through the low-loss interfaces based on the fs-laser inscribed 3D SiO_2 chip. The 3D SiO_2 chip not only demultiplexes multiple spatial/mode channels of SDM fibers into arrayed single-mode channels with low crosstalk, but also provides an interface for silicon chips with small spot sizes. Each-channel signals are

guided to the 2D silicon chip, where multiple on-chip channels can also be multiplexed in multimode waveguides. Each channel can be manipulated individually to control the wavelength/amplitude of the signals by reconfigurable optical add/drop multiplexer (ROADM) and Mach-Zehnder interferometer (MZI) array. Building on the synergistic optimization enabled by hybrid integration technology, diverse optical fibers, 3D SiO_2 chip, and 2D Si chip can be directly edge-coupled to leverage their respective strengths and compensate for their limitations. Based on this approach, the fiber-chip-fiber system facilitates multiple functionalities. 1) Structured light tailoring: the system enables arbitrary mode-field conversion not only between different fiber types but also from multiple SDM fibers to on-chip multimode waveguides. 2) Multi-dimensional signal management: a larger-scale 288-channel ROADM is employed to implement dynamic interconnections in an 8-core fiber, with an MZI array used for channel equalization. 3) High-capacity data transmission: a fiber-chip-fiber interconnection link incorporating OAMF, MCF, FMF and SMF is constructed, supporting 288 optical signal channels and achieving a system capacity of 30 Tbit/s.

In this work, the implementation setup of this concept is depicted in Fig. 2b. It comprises input/output fiber, add/drop fiber, 3D SiO_2 chip, 2D Si chip, printed circuit board (PCB). The inset of Fig. 2a shows the interface of input 8-core fiber in 3D SiO_2 chip. By using the high-repetition-rate Ytterbium-based laser that provides a fs-laser beam, these interfaces are fabricated in a footprint 20 × 30 mm^2 glass-substrate chip. Silicon chip is fabricated by the standard CMOS-compatible fabrication process with a 220 nm-thick silicon core. More details about the two fabrication methods can be found in Supplementary Information S1. Fig. 2c shows the photograph of silicon. The overall chip footprint is about 8 × 32 mm^2. Fig. 2d and Fig. 2e display the microring array, optical attenuation array, and crossing array. All of the tuning building blocks are wire-bonded to a carrier PCB and controlled by a programmable control circuit for reconfiguration. The scanning electron microscope images in Fig. 2f highlight the details of the edge coupler, the multimode interferometer, and the microring, respectively. In order to conveniently test individual add/drop channels, single-mode grating couplers are used to test each channel separately.

ARTICLE IN PRESS

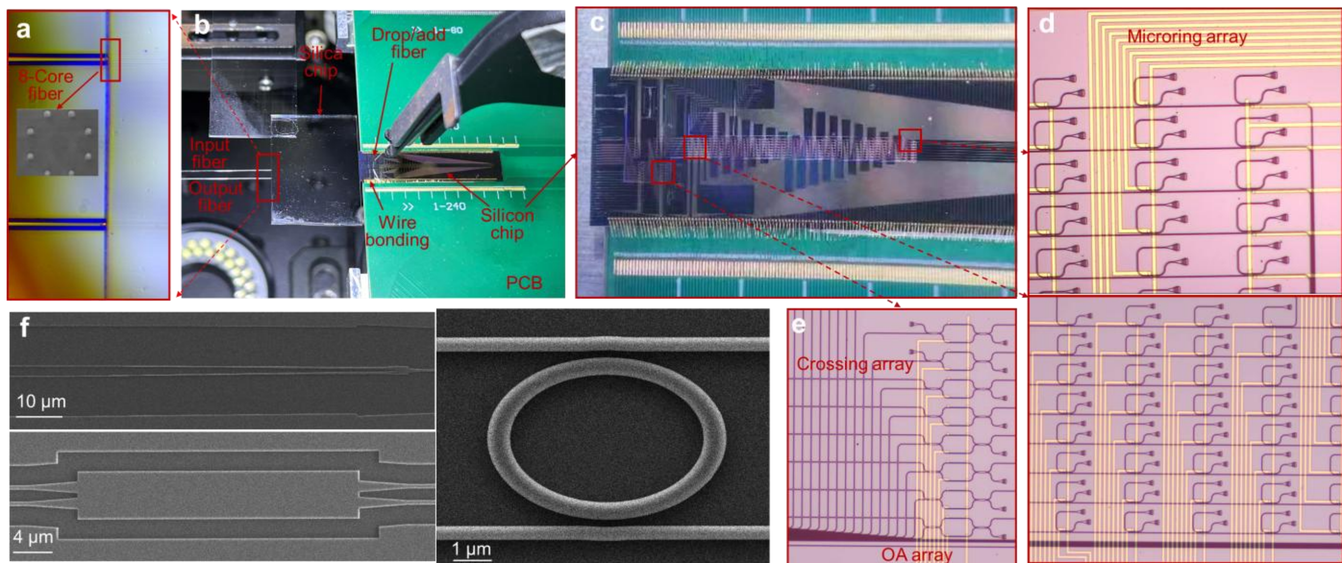

Fig. 2. Implementation setup of 3D/2D chip hybrid integration. a Input/output fibers and their interfaces in silica 3D chip. Inset is the interface of 8-core fiber. **b** Photograph of 3D/2D chip hybrid integration. **c** Photograph of silicon chip. **d** Optical microscopy images of microring array. **e** Optical microscopy images of optical attenuation array and crossing array. **f** Scanning electron micrographs of the silicon devices, showing the edge coupler, the multimode interferometer, and the microring.

ARTICLE IN PRESS

Structural light tailoring in fiber and chip

Due to the exceptional 3D fabrication capabilities of fs-lasers direct writing technology, the silica chip offers advantages in insertion loss, size, and flexibility, while also being highly versatile. It can efficiently tailor various optical fields in fiber with low loss and low crosstalk. Hence, arbitrary mode-field conversion can be realized by introducing several high-performance components. First, we use the slit method for beam shaping to improve the symmetry of the waveguide cross-section, thereby achieving ultra-low-loss waveguides. As shown in Fig. 3a, by fixing a mechanical slit above the objective lens, the waveguide shape can be transformed from a long and narrow form to an approximate circular shape. This improvement arises because the femtosecond laser emitted from the laser source does not exhibit a perfect Gaussian beam profile, which in turn affects the waveguide cross-section during fabrication. As shown in the transmission spectrum in Fig. 3a, the transmission loss of the waveguide is reduced by an order of magnitude, from 1 dB/cm to 0.1 dB/cm. Low-loss waveguides serve as the fundamental building blocks for low-loss 3D photonic devices. Then, for multi-core fiber mode-field transformation, S-bend

ARTICLE IN PRESS

waveguides are employed to distribute the spatial positions of the mode fields. An optimized bending curve is utilized to reduce mode leakage, inter-core crosstalk, and transmission loss of 3D device. As illustrated in Fig. 3b, the curvature of the bending curve is continuous, ensuring that the first and second derivatives of the waveguide's curvature function are continuous, theoretically reducing the transition loss to zero[39,40]. The detailed bending design process can be found in Supplementary Information S2. Based on the optimized S-bend waveguides, we fabricated high-performance 8-core MCF fan-in/fan-out (FIFO) devices. As depicted in the transmission spectrum in Fig. 3b, the device losses across the entire C-band for all channels is <2.7 dB. The crosstalk is <-36 dB across the C-band, as shown in Fig. S8. The transmission spectrum measurement setups for various devices can be found in Supplementary Information S3. Next, we utilize a photonic lantern structure to (de) multiplex various modes in MDM fibers. As shown in Fig. 3c, conventional photonic lanterns employ non-uniform waveguide designs due to varying waveguide diameters[41,42]. However, 3D waveguides are fabricated with a minimum loss diameter, and different waveguide diameters can degrade the performance of waveguide devices. Here, uniform waveguides and 3D trajectories are used to achieve low-loss, low-crosstalk FMF (de)multiplexing, by fully leveraging the 3D fabrication capabilities. Notably, we can achieve efficient, low-crosstalk OAM mode multiplexing and demultiplexing by modifying the parameters of the 3D trajectory. The designs for few-mode fiber and OAM fiber are detailed in Supplementary Information S4. Fig. 3c presents that the insertion loss for all channels is less than 3 dB. Notably, the loss of the fundamental mode in the multi-mode multiplexer is lower than the higher-order modes but noticeably higher than the loss for single-mode interfaces. As shown in the Supplementary Information S5 the corresponding mode multiplexers also exhibit crosstalk of <-15 dB, supporting high-speed optical communication. Finally, in addition to providing interfaces for various optical fibers, our 3D silica chip can also provide interfaces for silicon chips. As is well known, when single-mode coupling to the end face of a silicon chip, there is a significant size mismatch. Typically, lens fibers or tapered fibers are used to achieve a small mode-field spot size, reducing loss. Here, we utilize the fs laser to compress the spot size directly on the chip, as shown in Fig. 3d. Usually, single-mode waveguides are fabricated by multiple direct writing steps with slight offsets.

ARTICLE IN PRESS

In this case, we gradually focus the waveguide to a single point, thereby efficiently coupling it to the silicon chip. The transmission spectra in Fig. 3d show that the simulation and measurement coupling losses of the 2D/3D chip are lower than 1.6 dB and 2 dB in the C-band, respectively.

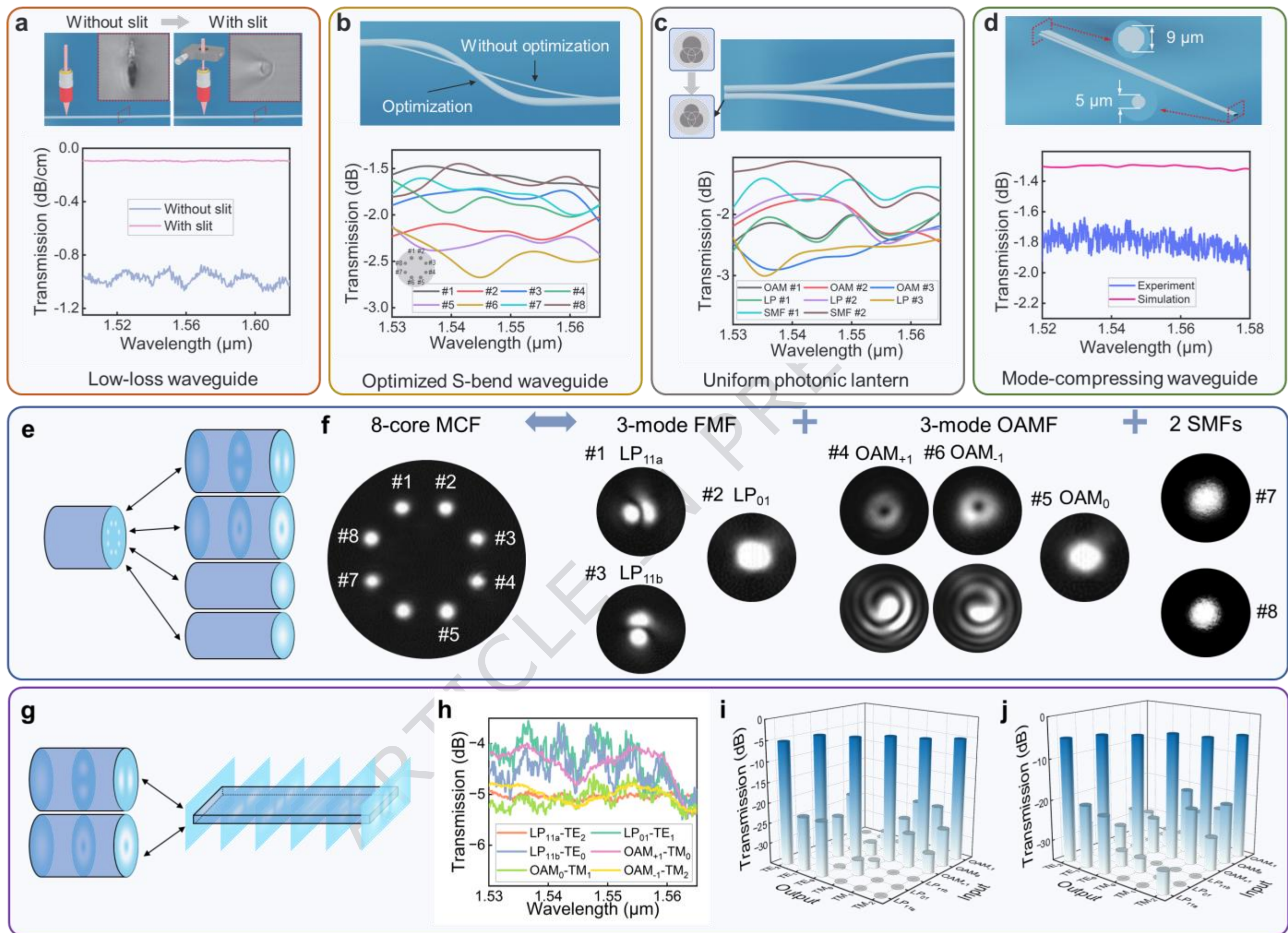

Fig. 3. Basic building blocks characteristics for structural light tailoring. a Fabrication diagram, waveguide cross section, and transmission spectra of the fs-laser inscribed 3D waveguide with or without slit. **b** Structural diagram of S-bend waveguide with or without optimization and measured transmission spectra of the 8-core FIFO coupler. **c** Structural concept of uniform photonics lantern and measured transmission spectra of the FMF/OAMF (de)multiplexers. **d** Structural diagram and transmission spectra of mode-compressing waveguide by using a taper structure in 3D photonics chip. **e** Conceptual drawings of mode-field conversion between 8-core MCF, 3-mode FMF, 3-mode OAMF, 2 SMFs. **f** Measured cross-section intensity profiles of the input 8-core MCF and output FMF

ARTICLE IN PRESS

(LP_{01}, LP_{11a}, LP_{11b}), 3-mode OAMF (OAM_0, OAM_1, OAM_{-1}), 2 SMFs. **g** Conceptual drawings, **h** measured transmission spectra, and **i,j** crosstalk matrix of mode-field conversion between fiber modes (LP_{01}, LP_{11a}, LP_{11b}, OAM_0, OAM_1, OAM_{-1}) and waveguide modes (TE_0, TE_1, TE_2, TM_0, TM_1, TM_2). **i,j** correspond to wavelengths of 1550nm and 1530nm respectively.

To demonstrate arbitrary structured light field conversion in optical fibers, we present in Fig. 3e a structural diagram of mode-field transformations among an 8-core MCF, 3-mode FMF (LP_{01}, LP_{11a}, LP_{11b}), 3-mode OAMF (OAM_0, OAM_1, OAM_{-1}), and 2 SMFs. Based on these fundamental building blocks, an integrated 3D silica photonic chip is fabricated incorporating an 8-core FIFO device, a 3-mode LP mode (de)multiplexer, a 3-mode OAM (de)multiplexer, and two single-mode interfaces. All multimode ports are located on one side of the chip, while the demultiplexed single-mode outputs are placed on the opposite side. The single-mode output ports are spaced at 127 μm, enabling efficient coupling with commercially available fiber arrays. Each single-mode port is equipped with a tapered waveguide to compress the mode field diameter, facilitating low-loss coupling with silicon waveguides. Notably, silicon waveguides can provide compact, low-loss 90° bending structures that are challenging to achieve in 3D glass-based platforms. As in our previous work[15], incorporating multi-channel non-blocking optical switches enables reconfigurable mapping and conversion of structured light fields. Thus, each core channel of the 8-core fiber can be dynamically mapped onto various higher-order or fundamental modes in other fibers. Tailored 3D chips can be designed and fabricated to enable the desired spatial light field conversion. Fig. 3f shows measured cross-sectional intensity profiles of the input 8-core MCF and output FMF, OAMF, and two SMFs. Interference patterns of the OAM modes are also included, confirming the device's ability to precisely manipulate and interconvert diverse structured optical fields among different fiber types. As shown in Fig. S10 (Supplementary Information S6), the transmission spectra for various fiber conversion exhibit an insertion loss less than 9 dB and crosstalk below –13 dB throughout the C-band.

Furthermore, as illustrated in Fig. 3g, our integrated devices allow for mode conversion not only between fibers but also between fibers and silicon multimode waveguides. With on-chip mode

ARTICLE IN PRESS

ARTICLE IN PRESS

(de)multiplexers, multiple structured light fields can be directly coupled into and out of silicon photonic circuits. The silicon multimode waveguide has a width of 1.2 μm and a height of 0.22 μm. Fig. 3h displays the transmission spectra of the three LP modes, three OAM modes, and six directly converted modes on-chip, showing insertion losses below 5.5 dB across the entire C-band. Fig. 3i and Fig. 3j report mode crosstalk levels below –13 dB at both 1530 nm and 1550 nm. Fig. S10 shows that crosstalk remains below –13 dB across other wavelengths, demonstrating broadband operational stability.

Large-scale multifunctional silicon chip

Silicon photonic signal managers, with their vast bandwidth, high refractive index contrast, compactness, and robust information security, have ushered in a new era of information management. With the aid of tunable components, programmable photonic signal managers can perform various signal management tasks, thereby establishing a multifunctional hardware platform. Among these components, the MZI, consisting of two 2×2 power splitters and a phase shifter, is one of the key tunable elements. It can be used to construct multi-channel optical switches[15], MIMO processors[16], unitary matrices, quantum gates[43], and more, thereby driving the miniaturization of fields such as optical communication, optical computing, and quantum computing. In this work, we employ the MZI as an optical attenuator array to achieve optical power balancing. Fig. 4a shows the measurement results of the MZI device, which demonstrate insertion loss of less than 1 dB and crosstalk below -22 dB. Based on this MZI array, we can also selectively attenuate different spatial channels. As illustrated in Fig. 4b, we can independently attenuate one channel, two channels, or four channels. In addition to managing spatial channels, the 2D silicon chip can also perform wavelength management using micro-ring resonators (MRRs) based on its own resonant characteristics. As shown in the inset of Fig. 4c, the wavelength-selective switch uses elliptical micro-rings with adiabatically varying radii and core widths[44]. In the coupling region, a relatively large bend radius and narrower waveguide width are designed to achieve sufficient coupling efficiency, while a smaller bend radius and wider core width are used to reduce bending losses and cavity length. The shortened cavity length helps achieve a free spectral range (FSR) of ~26 nm, supporting 36

ARTICLE IN PRESS

wavelengths with channel spacing of ~0.4 nm (~50 Ghz). Unlike traditional MRR optimized for critical coupling, this design slightly reduces the spacing between the coupling waveguides to enhance coupling efficiency, thereby achieving an "under-coupled" state. In this under-coupled state, the 3-dB bandwidth of the resonant peaks can be broadened with a slight sacrifice in insertion loss, facilitating higher-speed signal processing. A detailed 3-dB bandwidth analysis of the MRR is provided in Supplementary Information S7.

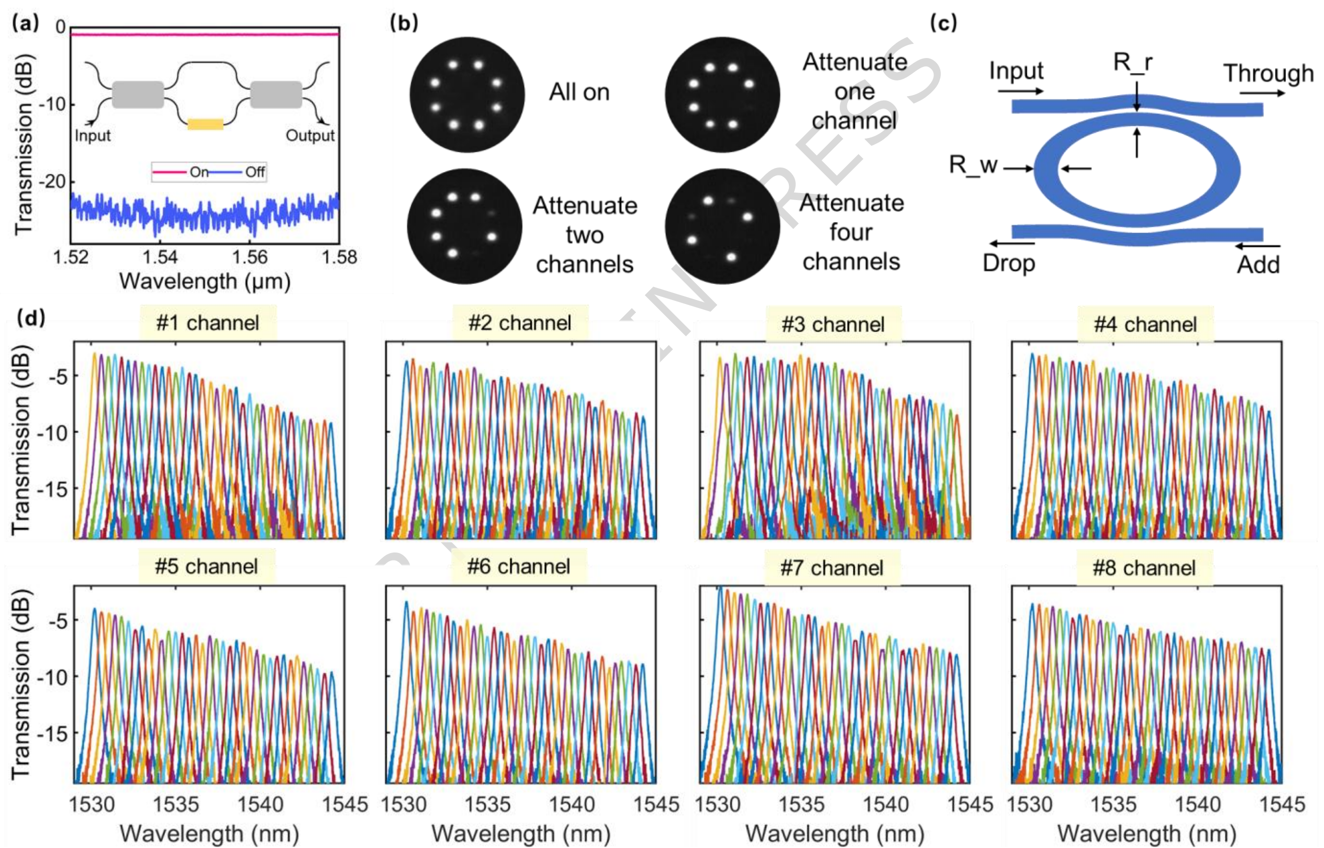

Fig 4. Large-scale 2D silicon ROADM. (**a**) Measured transmission spectra of MZI switch when the state is "on" or "off". The insets are the structural diagram. (**b**) Measured intensity profiles of 8-core fiber when zero, one, two, or four channels are attenuated. (**c**) Structural diagram of micro-ring resonator. (**d**) The measured drop spectra of eight arrays of 36 cascaded micro-ring resonators with thermo-optical tuning.

Fig. 4d displays the transmission spectra of 8 tuned micro-ring resonators within a 36 micro-ring array, demonstrating their ability to effectively manage signals across 288 wavelengths. The inconsistency in

ARTICLE IN PRESS

MRR insertion loss originates from two main factors. First, the cascaded structure inherently causes the loss at the resonant wavelength to increase along the chain. Second, the MRR insertion loss is extracted by subtracting the losses of other components from the total link loss, and the cumulative effect of fabrication-induced variations across different channels contributes to a power fluctuation of approximately 2 dB in the MRR response.

Diverse fiber-chip parallelization communications

Finally, we demonstrate an optical fiber-chip-fiber parallel communication system compatible with various fiber types. Based on these devices, we further build a diversified system, achieving 288-channel, 30 Tbit/s multidimensional data transmission and management. Figs. 5a-c show the complete experimental system for multidimensional data transmission and management, which consists of three main parts: a wavelength-division multiplexing (WDM) signal transmitter with 16-level quadrature amplitude modulation (QAM), the fiber/3D/2D hybrid integration system, and a coherent optical receiver followed by digital signal processing. At the transmission end, 36 wavelength-tunable external cavity lasers (ECLs) serve as the optical signal carriers, with wavelength spacing of 0.4 nm/50 GHz. To emulate practical communication scenarios, the 36 ECLs are divided into odd and even groups, and a four-channel arbitrary waveform generator (AWG: Keysight M8199A) is used to drive two in-phase/quadrature (I/Q) modulators to independently modulate 28-GBaud 16-QAM signals. To prevent the underestimation of bit-error rate (BER) in the WDM system, an optical delay line is employed to decorrelate the odd and even optical signals. Alternatively, a 100G optical frequency comb can be used between the two channels to reduce the size of the transmitter. The modulated odd and even signals are combined through a 50:50 optical coupler (OC) and amplified by a C-band EDFA. Subsequently, the 36-channel WDM signals (wavelength range from 1530.2 nm to 1544.2 nm) are transmitted to the FMF-chip data transmission and signal management system, as shown in Fig. 5d. The observed non-uniform channel spacing, resulting from laser tuning inaccuracies, directly contributes to performance fluctuations in inter-wavelength crosstalk and BER. The amplified WDM signal is divided into eight parts and further decorrelated via

ARTICLE IN PRESS

ARTICLE IN PRESS

different optical delay lines. Eight EDFAs are used to compensate for the losses in the fiber-chip-fiber system. The maximum loss for the dropping function system is 25 dB, consisting of the following components: a silica fan-in chip (< 3 dB), an 8-core fiber segment (< 1 dB), a hybrid integrated coupler (< 4.5 dB), a silicon MZI (< 1 dB), an MRR array (< 9 dB), a grating (< 4.5 dB), and multiple bends and crossings (< 2 dB). For the adding function system, the maximum loss is 27.5 dB. Compared to the dropping system, the adding system exhibits an extra 2.5-dB loss due to the 1.2-cm-long waveguide loop integrated in the silicon chip. These eight channels are multiplexed into eight different cores of an 8-core fiber using silica photonic FIFO devices. After transmission through the 8-core fiber, the high-capacity signal is coupled into the silicon chip using customized edge couplers. Next, an MZI switch array is used to balance channel losses. Therefore, the 288-channel signals can be flexibly extracted from the 2D photonic integrated circuits and sent to the integrated coherent optical receiver and local oscillator (LO). A real-time oscilloscope (Keysight UXR0594) is used to sample and store electrical signals from the coherent optical receiver for offline DSP and BER evaluation. The offline DSP includes signal resampling, IQ non-orthogonal compensation using the Gram-Schmidt orthogonalization process, linear equalization, frequency offset estimation and carrier phase recovery. In addition to signal dropping, external signals can also be added to the communication system through micro-ring resonators. Similarly, the MZI array, acting as an equalizer, can manage signals in individual spatial channels. Finally, the signals from these eight spatial channels can not only be coupled into the eight-core fiber through the 8-core-fiber FIFO devices but also be coupled into different fibers through the fiber/3D/2D hybrid integration coupler (3 LP modes, 3 OAM modes, 2 base modes). Notably, only two fixtures are used to secure two fibers (one input, one output), but in practice, more fiber arrays can be provided to customize multi-fiber input-output systems.

To demonstrate the data throughput, we asynchronously demultiplexed, received, and tested each spatial/wavelength channel in the multi-fiber/3D/2D hybrid integration fiber-chip system. Fig. 5e shows the BER test results for all 288 channels in the 8-core fiber data transmission and management scenario. The results show that the BER for each channel is below the 7% forward error correction (FEC) threshold

ARTICLE IN PRESS

ARTICLE IN PRESS

of 3.8×10^{-3}. Fig. 5f shows the relationship between the BER and the received optical signal-to-noise ratio (OSNR) for the eight different wavelength spatial channels extracted from the silicon ROADM system. To simplify and ensure comprehensiveness, we select six mode channels: #8 (channel 1), #7 (channel 6), #6 (channel 11), #5 (channel 16), #4 (channel 21), #3 (channel 26), #2 (channel 31), and #1 (channel 36). It is clear that the BER curves for these six selected channels consistently stay below the 7% FEC threshold, even in the presence of mode-to-mode and wavelength-to-wavelength crosstalk. When the OSNR exceeds 21 dB, the performance remains stable. Compared to the backhaul transmission performance of each channel, the OSNR penalty for the six selected channels in the FMF-chip system is less than 5 dB under the 7% FEC threshold. For the adding functionality, we choose a multi-fiber scenario to demonstrate the observed OSNR penalty, with results showing that the penalty for all eight spatial channels remains below 7 dB, as shown in Fig. 5g. Notably, the OSNR penalty for the base mode channels is slightly lower than that for the higher-order mode channels due to increased mode crosstalk in the latter. Fig. 5h presents the BER test results for all 288 channels in the multi-fiber data transmission and management scenario, showing that all BER values remain below the 7% FEC threshold. The inset shows the typical constellation diagram for the 16-QAM signal, highlighting the excellent performance. Therefore, the proposed multi-fiber data transmission and signal management system successfully achieve total transmission rate of 30.15 Tbit/s (28 Gbaud × 4 bits per symbol × 8 spatial modes × 36 wavelengths / (1 + 7%) ≈ 30.15 Tbit/s).

ARTICLE IN PRESS

ARTICLE IN PRESS

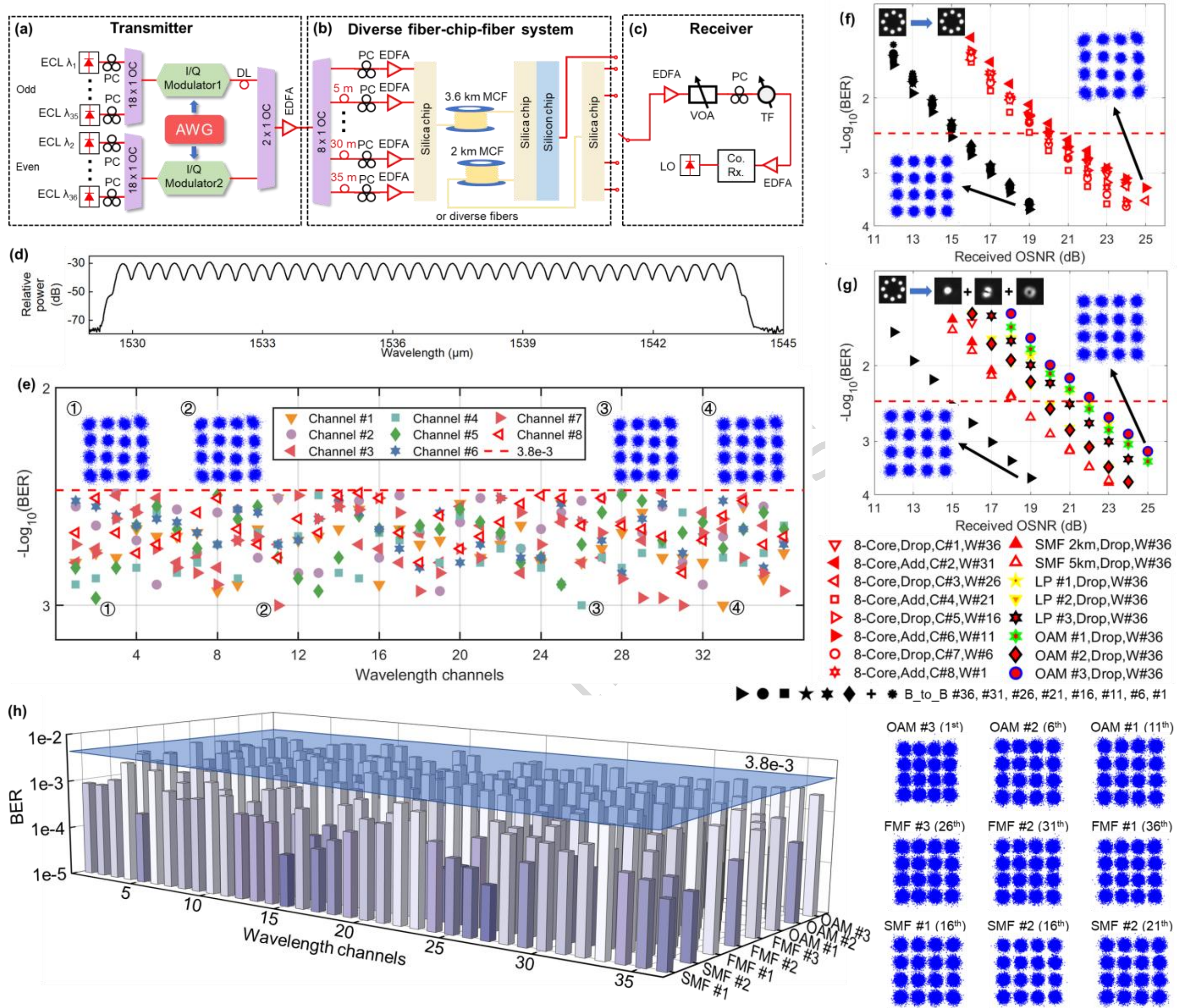

Fig. 5. Diverse fiber-chip parallelization communications. The experimental setup for (**a**) the transmitter, (**b**) the diverse fiber-chip parallelization system and (**c**) the receiver. (**d**) An optical spectrum of 36-wavelength WDM signals with ~ 50 G channels spacing (from 1530.2 nm to 1544.2 nm). (**e**) The measured BERs of all 288 dropping channels for dropping function. (**f**) Measured BER vs. OSNR curves for 8 cores of different wavelengths. (**h**) The measured BERs of all 288 dropping channels for adding function. (**g**) Measured BER vs. OSNR curves for 8 spatial channels of different wavelengths. The inserts in (**e**) - (**h**) are the typical constellations of 16-QAM signals. ECL: External cavity laser; DL: Delay line; PC: Polarization controller; OC: Optical coupler; AWG: Arbitrary waveform

generator; EDFA: Erbium-doped fiber amplifier; VOA: Variable optical attenuator; TF: tunable filter; Co.Rx.: coherent receiver; LO: local oscillator.

Discussion

In summary, we have proposed a diverse fiber/3D/2D hybrid integration solution that enables direct interfacing between various fibers and chips. Due to the 3D processing capabilities of femtosecond lasers, the SiO_2 structures we fabricated can precisely cut high-performance SDM fiber interfaces, as well as provide low-loss interfaces for silicon photonic chips. This fiber/3D/2D hybrid integration not only facilitates the easy conversion of modes within fibers but also enables the conversion between fibers and chip multimode waveguides. Additionally, we have fabricated a large-scale, multifunctional 2D silicon chip to manage spatial and wavelength signals, featuring 288 signal channels. With these key components, we construct a diverse fiber-chip-fiber parallelization communication system that is compatible with multi-core fibers, few-mode fibers, vortex fibers, and single-mode fibers. By transmitting 28-Gbaud 16-QAM signals, our diversified fiber-chip system achieves a groundbreaking data transmission and management capability of 30 Tbit/s. We believe this demonstration provides a scalable architecture for multidimensional data transmission and management in next-generation optical communications.

ARTICLE IN PRESS

While this fiber-chip optical transmission and management system has achieved significant increases in channel count and system capacity, it still falls far short of the scale and capacity of multi-dimensional optical transmission systems using bulk components[11,45–49]. A detailed comparison of the tables can be found in Supplementary Information S8. Looking ahead, with the continuous advancement of integrated photonic technologies, the throughput of fiber-chip interfaces and photonic processing devices holds the potential to eventually rival the capacity of optical transmission systems based on bulk optical components. Realizing direct and efficient interconnection between various optical fibers and silicon chips requires the development of a greater number and higher-order (de)multiplexers, minimizing

ARTICLE IN PRESS

channel loss and crosstalk. For the approach that increases channel count via core-division multiplexing, 3D silica chips can leverage the excellent fabrication capabilities of femtosecond laser direct writing technology to realize FIFO device for high-core-count fibers (e.g., 19-core or 24-core fibers)[50,51]. Higher-order mode multiplexer can be implemented through specialized structural designs[52,53]. Managing such a large number of channels requires more optical management equipment, which may necessitate further improvements in the performance of integrated optical management components. In the wavelength dimension, parameter optimization is expected to allow 3D silica devices to operate across the entire C+L band. Furthermore, the smallest reported MRR currently shows a FSR of 93 nm, enabling the process of more wavelengths through cascading[54]. Crucially, the design of the silicon chip can be optimized to eliminate polarization dependency, achieving polarization-independent optical management and thereby increasing the overall data throughput[55]. Therefore, by integrating these numerous cutting-edge technologies, the realization of Pbit/s fiber-chip optical transmission and processing systems is a foreseeable prospect.

Real-time configuration of silicon photonic processors is crucial for fiber-optic communication systems, as the demands of optical clients dynamically adjust according to practical applications and varying external environments[56]. Under conditions of slight disturbances, the mode and polarization dimensions in optical fibers exhibit greater sensitivity than the wavelength dimension: disturbances readily induce optical power coupling between spatial modes, leading to inter-mode crosstalk and altered dispersion properties. Such disturbances can trigger dynamic polarization mode dispersion and rapid polarization state rotation, resulting in failure of polarization demultiplexing at the receiver and decision errors. The combined effect of these factors significantly increases the BER, thereby limiting communication transmission capacity. Fortunately, the progressive self-configuration method with feedback has been demonstrated to be a straightforward and efficient approach for demodulating single-fiber optical fields [57,58]. This method is capable of handling arbitrary mode evolution and polarization rotation following fiber transmission. Notably, when employing thermo-optic phase shifters, the configuration speed of photonic processors can reach approximately 10 microseconds[59,60], while the use of electro-optic phase shifters

ARTICLE IN PRESS

enables sub-nanosecond reconfiguration speeds. These advances pave the way for the future real-time management of high-dimensional fiber systems through integrated photonic processors, offering a promising solution to address dynamic fiber disturbances[61].

Methods

Femtosecond-laser fabrication. The 3D silica chip is processed using femtosecond laser fabrication technology, employing a high-repetition-rate Ytterbium-based laser (wavelength: 1030 nm, repetition rate: 200 kHz, pulse duration: 234 fs). The femtosecond-laser, with linear polarization, is focused vertically approximately 50 μm below the top surface of the silica photonic chip using a 50× 0.42 objective lens. A linear slit is used to modify the laser beam profile, enabling the inscription of low-loss circular waveguides in the glass. Additionally, waveguides with multiple scanning passes are introduced to enhance the refractive index contrast and improve the waveguide's smoothness. The femtosecond-laser inscription speed is maintained at a constant rate of 0.2 mm/s. The refractive index contrast of the resulting waveguides is approximately 0.3%.

ARTICLE IN PRESS

Silicon chip Fabrication. The 2D silicon photonic chip is fabricated using a CMOS-compatible process on a silicon-on-insulator (SOI) substrate, which features a 220-nm-thick top silicon layer and a 2-μm-thick buried oxide layer. Device patterns are defined using electron-beam lithography (EBL), followed by dry reactive-ion etching to achieve etch depths of 70 nm and 220 nm. A 1.2-μm-thick SiO_2 cladding layer is then deposited to protect the photonic circuits. For metallization, a titanium (Ti) layer is used for local heat generation, while aluminum is employed for electrical signal routing. To protect the electrode pads, an additional SiO_2 layer is deposited, and a final set of deep ultraviolet (DUV) lithography and reactive ion etching (RIE) processes are applied to remove the dielectric material from the pads.

Measurements. For multimode silicon devices on the chip, a set of mode multiplexers and demultiplexers are used to prepare and demodulate higher-order waveguide modes. These mode

ARTICLE IN PRESS

multiplexers/demultiplexers are similar to other single-mode devices and are interconnected with single-mode fibers through either end-face coupling or grating couplers. For 3D SiO_2 chips, devices with multimode ports require two identical devices and shorter fibers to form an interconnection system for testing. For devices containing only single-mode channels, measurements are taken via single-mode end-face coupling. In all chip tests, a tunable laser (Santec TSL-710) is used as the light source, covering the C-band, and its polarization state is adjusted using a polarization controller. Finally, the optical signal is monitored using an optical power meter (PMSII-A). The detailed setup information can be found in Supplementary Information S3.

ARTICLE IN PRESS

Data availability: The data that supports the plots within this paper and other findings of this study are available on Zenodo (https://doi.org/10.5281/zenodo.18241349). All other data used in this study are available from the corresponding authors upon request.

References

1. Richardson, D. J. Filling the Light Pipe. *Science* **330**, 327–328 (2010).

2. Tkach, R. W. Scaling optical communications for the next decade and beyond. *Bell Labs Tech. J.* **14**, 3–9 (2010).

3. Cheng, Q., Bahadori, M., Glick, M., Rumley, S. & Bergman, K. Recent advances in optical technologies for data centers: a review. *Optica* **5**, 1354 (2018).

4. Pan, T. *et al.* Non-orthogonal optical multiplexing empowered by deep learning. *Nat Commun* **15**, 1580 (2024).

5. Chen, Z.-Y. Use of polarization freedom beyond polarization-division multiplexing to support high-speed and spectral-efficient data transmission.

ARTICLE IN PRESS

6. Su, Y., He, Y., Chen, H., Li, X. & Li, G. Perspective on mode-division multiplexing. *Applied Physics Letters* **118**, 200502 (2021).

7. Winzer, P. J. Making spatial multiplexing a reality. *Nature Photon* **8**, 345–348 (2014).

8. Richardson, D. J., Fini, J. M. & Nelson, L. E. Space-division multiplexing in optical fibres. *Nature Photon* **7**, 354–362 (2013).

9. Puttnam, B. J., Rademacher, G. & Luís, R. S. Space-division multiplexing for optical fiber communications. *Optica* **8**, 1186 (2021).

10. Van Uden, R. G. H. *et al.* Ultra-high-density spatial division multiplexing with a few-mode multicore fibre. *Nature Photon* **8**, 865–870 (2014).

11. Rademacher, G. *et al.* Peta-bit-per-second optical communications system using a standard cladding diameter 15-mode fiber. *Nat Commun* **12**, 4238 (2021).

12. Essiambre, R.-J. & Tkach, R. W. Capacity Trends and Limits of Optical Communication Networks. *Proc. IEEE* **100**, 1035–1055 (2012).

13. Essiambre, R.-J., Kramer, G., Winzer, P. J., Foschini, G. J. & Goebel, B. Capacity Limits of Optical Fiber Networks. *J. Lightwave Technol.* **28**, 662–701 (2010).

14. Li, K. *et al.* Fiber–Chip–Fiber Mode/Polarization/Wavelength Transmission and Processing with Few-Mode Fiber, (de)Multiplexing SiO_2 Chip and ROADM Si Chip. *Laser & Photonics Reviews* **18**, 2300489 (2024).

15. Li, K. *et al.* Handling mode and polarization in fiber by fs-laser inscribed (de)multiplexer and silicon switch array. *PhotoniX* **4**, 14 (2023).

ARTICLE IN PRESS

ARTICLE IN PRESS

16. Lu, K. *et al.* Empowering high-dimensional optical fiber communications with integrated photonic processors. *Nat Commun* **15**, 3515 (2024).

17. Hayashi, T., Taru, T., Shimakawa, O., Sasaki, T. & Sasaoka, E. Design and fabrication of ultra-low crosstalk and low-loss multi-core fiber. (2011).

18. Wang, J. & Zhang, X. Orbital Angular Momentum in Fibers. *J. Lightwave Technol.* **41**, 1934–1962 (2023).

19. Wang, J., Chen, S. & Liu, J. Orbital angular momentum communications based on standard multi-mode fiber (invited paper). *APL Photonics* **6**, 060804 (2021).

20. Atabaki, A. H. *et al.* Integrating photonics with silicon nanoelectronics for the next generation of systems on a chip. *Nature* **556**, 349–354 (2018).

21. He, Y. *et al.* On-chip metamaterial-enabled high-order mode-division multiplexing. *Adv. Photon.* **5**, (2023).

22. Luo, L.-W. *et al.* WDM-compatible mode-division multiplexing on a silicon chip. *Nat Commun* **5**, 3069 (2014).

23. Dai, D., Wang, J., Chen, S., Wang, S. & He, S. Monolithically integrated 64-channel silicon hybrid demultiplexer enabling simultaneous wavelength- and mode-division-multiplexing: Monolithically integrated 64-channel silicon hybrid demultiplexer. *Laser & Photonics Reviews* **9**, 339–344 (2015).

24. Li, K., Cao, X., Wan, Y., Wu, G. & Wang, J. Fundamental analyses of fabrication-tolerant high-performance silicon mode (de)multiplexer. *Opt. Express* **30**, 22649 (2022).

25. Dai, D. *et al.* 10-Channel Mode (de)multiplexer with Dual Polarizations. *Laser & Photonics Reviews* **12**, 1700109 (2018).

ARTICLE IN PRESS

ARTICLE IN PRESS

26. Forbes, A., Dudley, A. & McLaren, M. Creation and detection of optical modes with spatial light modulators. *Adv. Opt. Photon.* **8**, 200 (2016).

27. Li, S., Mo, Q., Hu, X., Du, C. & Wang, J. Controllable all-fiber orbital angular momentum mode converter. *Opt. Lett.* **40**, 4376 (2015).

28. Li, K., Cao, X. & Wang, J. Broadband and efficient multi-mode fiber-chip edge coupler on a silicon platform assisted with a nano-slot waveguide. *Opt. Express* **30**, 47249 (2022).

29. Zhang, R. *et al.* Ultra-High Bandwidth Density and Power Efficiency Chip-To-Chip Multimode Transmission through a Rectangular Core Few-Mode Fiber. *Laser & Photonics Reviews* **17**, 2200750 (2023).

30. Jimenez Gordillo, O. A. *et al.* Fiber-Chip Link via Mode Division Multiplexing. *IEEE Photon. Technol. Lett.* **35**, 1071–1074 (2023).

31. Marchetti, R., Lacava, C., Carroll, L., Gradkowski, K. & Minzioni, P. Coupling strategies for silicon photonics integrated chips [Invited]. *Photon. Res.* **7**, 201 (2019).

32. Zhou, X., Yi, D., Chan, D. W. U. & Tsang, H. K. Silicon photonics for high-speed communications and photonic signal processing. *npj Nanophoton.* **1**, 27 (2024).

33. Zhou, X. *et al.* Fully Etched Low-Back-Reflection and High-Efficiency Silicon Waveguide Grating Couplers with Minimum feature size above 260 nm. *J. Lightwave Technol.* 1–6 (2025) doi:10.1109/JLT.2024.3524298.

34. Tong, Y., Zhou, W., Wu, X. & Tsang, H. K. Efficient Mode Multiplexer for Few-Mode Fibers Using Integrated Silicon-on-Insulator Waveguide Grating Coupler. *IEEE J. Quantum Electron.* **56**, 1–7 (2020).

ARTICLE IN PRESS

ARTICLE IN PRESS

35. Shen, W., Du, J., Xiong, J., Ma, L. & He, Z. Silicon-integrated dual-mode fiber-to-chip edge coupler for 2 × 100 Gbps/lambda MDM optical interconnection. *Opt. Express* **28**, 33254 (2020).

36. Yang, K. Y. *et al.* Multi-dimensional data transmission using inverse-designed silicon photonics and microcombs. *Nat Commun* **13**, 7862 (2022).

37. Watanabe, T. *et al.* Coherent few mode demultiplexer realized as a 2D grating coupler array in silicon. *Opt. Express* **28**, 36009 (2020).

38. Kuo, P.-C. *et al.* 4.36 Tbit/s Silicon Chip-to-Chip Transmission via Few-Mode Fiber (FMF) using 2D Sub-wavelength Grating Couplers. in *Optical Fiber Communication Conference (OFC) 2021* M3D.6 (Optica Publishing Group, Washington, DC, 2021). doi:10.1364/OFC.2021.M3D.6.

39. Fang, J. *et al.* 3D waveguide device for few-mode multi-core fiber optical communications. *Photon. Res.* **10**, 2677 (2022).

40. Kumar, V. & Priye, V. 3-D Multilayer S-Bend Silicon Waveguide Optical Interconnect. *IEEE Photon. Technol. Lett.* **30**, 1040–1043 (2018).

41. Chen, H. *et al.* Design Constraints of Photonic-Lantern Spatial Multiplexer Based on Laser-Inscribed 3-D Waveguide Technology. *J. Lightwave Technol.* **33**, 1147–1154 (2015).

42. Gross, S., Riesen, N., Love, J. D. & Withford, M. J. Three-dimensional ultra-broadband integrated tapered mode multiplexers: Three-dimensional ultra-broadband integrated tapered mode multiplexers. *Laser & Photonics Reviews* **8**, L81–L85 (2014).

43. SeyedinNavadeh, S. *et al.* Determining the optimal communication channels of arbitrary optical systems using integrated photonic processors. *Nat. Photon.* **18**, 149–155 (2024).

ARTICLE IN PRESS

ARTICLE IN PRESS

44. Liu, D., Zhang, L., Tan, Y. & Dai, D. High-Order Adiabatic Elliptical-Microring Filter with an Ultra-Large Free-Spectral-Range. *J. Lightwave Technol.* **39**, 5910–5916 (2021).

45. Soma, D. *et al.* 2.05 Peta-bit/s super-nyquist-WDM SDM transmission using 9.8-km 6-mode 19-core fiber in full C band. in *2015 European Conference on Optical Communication (ECOC)* 1–3 (IEEE, Valencia, Spain, 2015). doi:10.1109/ECOC.2015.7341686.

46. Soma, D. *et al.* 10.16-Peta-bit/s Dense SDM/WDM Transmission over 6-Mode 19-Core Fiber across the C+L Band. *J. Lightwave Technol.* 1–1 (2018) doi:10.1109/JLT.2018.2799380.

47. Luis, R. S. *et al.* 1.2 Pb/s Throughput Transmission Using a 160 μm Cladding, 4-Core, 3-Mode Fiber. *J. Lightwave Technol.* **37**, 1798–1804 (2019).

48. Rademacher, G. *et al.* 10.66 Peta-Bit/s Transmission over a 38-Core-Three-Mode Fiber. in *Optical Fiber Communication Conference (OFC) 2020* Th3H.1 (Optica Publishing Group, San Diego, California, 2020). doi:10.1364/OFC.2020.Th3H.1.

49. Liu, J. *et al.* 1-Pbps orbital angular momentum fibre-optic transmission. *Light Sci Appl* **11**, 202 (2022).

50. Liang, Y. *et al.* Low-insertion-loss femtosecond laser-inscribed three-dimensional high-density mux/demux devices. *Adv. Photon. Nexus* **2**, (2023).

51. Yan, G. *et al.* Spatial-division multiplexing self-homodyne coherent transmission over 19-/24-core fibers assisted by homemade fan-in/fan-out 3D photonic devices. *Opt. Express* **32**, 47982 (2024).

52. Wang, Y. *et al.* Precise mode control of laser-written waveguides for broadband, low-dispersion 3D integrated optics. *Light Sci Appl* **13**, 130 (2024).

ARTICLE IN PRESS

ARTICLE IN PRESS

53. Chen, Y. *et al.* Vector Vortex Beam Emitter Embedded in a Photonic Chip. *Phys. Rev. Lett.* **124**, 153601 (2020).

54. Liu, D., Zhang, C., Liang, D. & Dai, D. Submicron-resonator-based add-drop optical filter with an ultra-large free spectral range. *Opt. Express* **27**, 416 (2019).

55. Jiao, X. *et al.* Polarization-insensitive thermo-optic Mach–Zehnder switches on silicon. *Opt. Lett.* **49**, 7090 (2024).

56. Wang, H., Ai, J., Ma, Z., Ramachandran, S. & Wang, J. Finding the superior mode basis for mode-division multiplexing: a comparison of spatial modes in air-core fiber. *Adv. Photon.* **5**, (2023).

57. Annoni, A. *et al.* Unscrambling light—automatically undoing strong mixing between modes. *Light Sci Appl* **6**, e17110–e17110 (2017).

58. Milanizadeh, M. *et al.* Separating arbitrary free-space beams with an integrated photonic processor. *Light Sci Appl* **11**, 197 (2022).

59. Wang, H. *et al.* Ultracompact topological photonic switch based on valley-vortex-enhanced high-efficiency phase shift. *Light Sci Appl* **11**, 292 (2022).

60. Wang, J. *et al.* Ultrahigh extinction ratio and a low power silicon thermo-optic switch. *Opt. Lett.* **49**, 2705 (2024).

61. Rahim, A. *et al.* Taking silicon photonics modulators to a higher performance level: state-of-the-art and a review of new technologies. *Adv. Photon.* **3**, (2021).

ARTICLE IN PRESS

Acknowledgments

ARTICLE IN PRESS

This work is supported by the National Key R&D Program of China (2025YFE0102200(J.W.)), the National Natural Science Foundation of China (NSFC) (62125503, 62261160388(J.W.)), the Natural Science Foundation of Hubei Province of China (2023AFA028(J.W.)), the Technology Innovation Program of Hubei Province (Major Science and Technology Project) (2024BAA001(J.W.)), the Hubei Optical Fundamental Research Center (HBO2025TQ004(J.W.)), the High Quality Development Special Project of the Ministry of Industry and Information Technology(J.W.) ,and the China Association for Science and Technology Youth Talent Support Engineering Doctoral Program(K.L.).

Author contributions:

J.W. developed the concept. J.W., K.L., and C.C. conceived the experiment. J.W. provided experimental conditions. G.Y., C.C., K.L., G. W., H. C., and B.H. performed the experiment and acquired the experimental data. K.L., C.C. and J.W. carried out the data analyses. C.C. provided the silica chip. K.L. and J.W. wrote the original manuscript. All authors contributed to revising the paper. J.W. and K. L. finalized the paper. J.W. supervised the project.

Competing interests: All other authors declare they have no competing interests.

ARTICLE IN PRESS

Editorial Summary:

This work enables seamless fiber-to-fiber and fiber-to-chip mode-field conversions and establishes a universal multi-dimensional parallel communication architecture for next-generation high-capacity data transmission and management.

Peer review information: *Nature Communications* thanks the anonymous reviewer(s) for their contribution to the peer review of this work. A peer review file is available.